Solar Radiation in Summertime Arctic Stratus Clouds

GERALD F. HERMAN[1]

Space Science and Engineering Center, The University of Wisconsin, Madison 53706

(Manuscript received 4 February 1977, in revised form 5 May 1977)

ABSTRACT

The results are reported of pyranometric measurements of solar radiation in Arctic stratus decks made from aircraft flights over the Beaufort Sea during late July 1975. The reflectance of these cloud layers was nearly constant over the range of cloud thicknesses investigated, indicating the importance of the high surface reflectivity. The following ranges of reflectance are obtained: over the total solar spectrum, 60–75%; visible spectrum, 70–85%; near-infrared, 50–65%. Transmittances for the cloud layers are presented as a function of cloud geometrical depth, and the bulk absorptance averaged over all cloud decks was 7% in the total solar spectrum, and 5% and 9% in the visible and near-infrared, respectively.

Additional cloud parameters, namely, single scatter albedo $\tilde{\omega}_\nu$ and absorption optical depth τ_ν are derived by fitting the upward and downward flux profiles from each flight to a two-stream approximation to estimate the absorption optical depth. By assuming a linear relation between absorption optical depth and cloud thickness, the scattering parameter β_ν, which defines the increased path length caused by multiple scattering, is determined from a best fit to the complete set of observed reflectances and transmittances. The following ranges of β_ν are estimated: total solar, 8.75–10.7; visible, 9.01–14.3; near-infrared, 6.86–8.12. By assuming an asymmetry factor of 0.85 these values of β_ν yield estimates of the single scattering albedo (ω_ν) of 0.994–0.996 over the total solar spectrum, 0.994–0.998 in the visible, and 0.990–0.993 in the near-infrared. Examples are presented of cloud absorption calculated with these derived values of $\tilde{\omega}_\nu$.

1. Introduction

Very little is known about the optical properties of Arctic stratus clouds, and surprisingly few measurements have been made of solar radiation in stratus clouds in general. The importance of Arctic stratus in terms of the heat balance of the central Arctic is well appreciated (see, e.g., Vowinckel and Orvig, 1970) and attempts have been made to model the radiative (Wiscombe, 1973) and dynamical (Herman and Goody, 1976) properties of the cloud layers. Present understanding of real cloud radiative properties has depended for the most part on extensive surface-based observations (e.g., Marshunova, 1961; Vowinckel and Orvig, 1962; Gavrilova, 1963).

This paper presents results of solar radiation measurements made with Eppley pyranometers on board the NCAR *Electra*. Data were collected in six stratus cloud situations over the Beaufort Sea during July 1975 as part of the Arctic Ice Dynamics Joint Experiment (AIDJEX) field program. The goal of the experiment was to measure the *bulk* radiative properties of the clouds (reflectance and transmittance) and infer from them parameters necessary to calculate the disposition of solar radiation under specified conditions, *viz.*, single scatter albedo and optical depth. The experimental procedure closely parallels those of investigators in subtropical stratocumulus situations (Neiburger, 1949; Paltridge, 1971; Reynolds *et al.*, 1975) and in mid-latitude stratus (Robinson, 1958; Griggs, 1968).

2. Experimental program

a. Flight procedure

The data were collected during the two "radiation missions" of the AIDJEX aircraft program on 24 and 27 July 1976. Details of these profiles are given in Table 1 and the flight geometry is summarized in Fig. 1.

The selection of stratus layers suitable for profiling was a difficult task, and the decision to conduct a

TABLE 1. Radiation profiles.

Profile	Date (1976)	Location	Time (GMT)
A	24 July	73°03′N, 149°27′W	2023–2150
B	24 July	72°51′N, 150°00′W	2155–2250
C	24 July	72°39′N, 149°54′W	2256–2410
D	27 July	71°51′N, 149°18′W	2023–2155
E	27 July	72°30′N, 150°15′W	2306–2343
F	27 July	71°45′N, 150°15′W	2350–2425

[1] Present affiliation: Department of Meteorology, University of Wisconsin, Madison.

flight was based on information relayed to Barrow, Alaska, from the NOAA satellite receiving station near Fairbanks, and Flight Weather Services in Fairbanks and Barrow. The number of acceptable stratus days was surprisingly small, and in fact other studies seem to indicate that during mid-summer 1975 the Beaufort Sea experienced anomalously low occurrences of stratus cloud. Final selection of cloud strata in which to do vertical profiling was determined on the basis of visual observations of cloud horizontal extent, relative horizontal homogeneity, and absence of middle and upper level cloud forms which might contaminate the downward flux measurements. The data were apparently free of cirrus effects, but the the constraint of horizontal homogeneity was difficult to satisfy due to small-scale variations ($\leqslant 0.5$ km) in cloud geometry. Horizontal cloud extent ranged from 15 to more than 40 km and sampling time from 3 to 10 min per flight leg.

Experiments were scheduled to occur symmetrically about local solar noon to minimize errors due to varying solar elevation. During the flights the solar

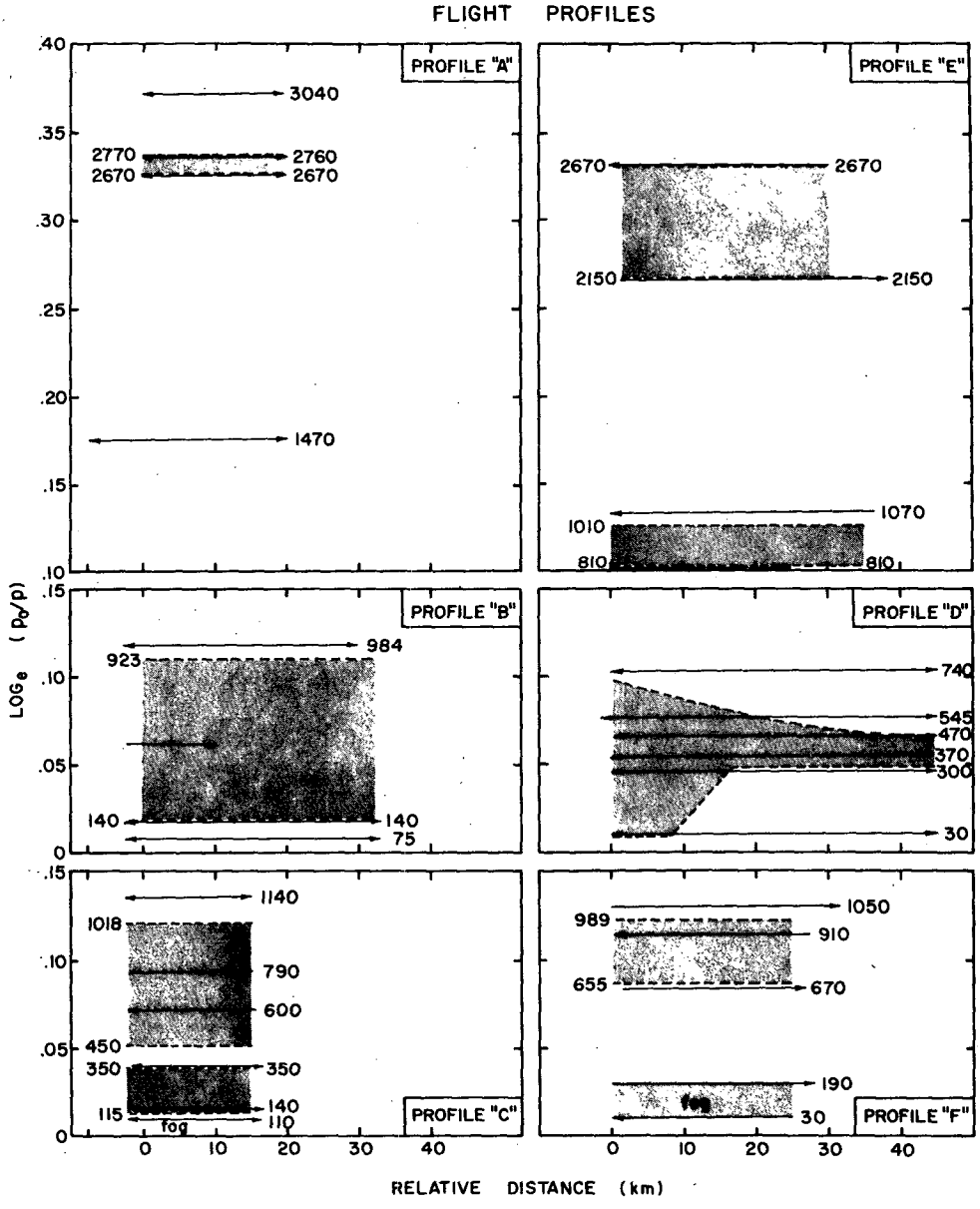

FIG. 1. Cloud geometry for Arctic stratus during AIDJEX radiation missions. Arrows directed toward the right or left denote legs flown into the sun or away from the sun, respectively. Values to the right denote approximate flight altitudes (m), while values to the left are estimates of cloud top or base. Length of arrows denotes length of flight leg. Shading denotes thickness only and does not indicate cloud horizontal extent.

zenith angle ranged from ~54° at local noon to 67° at 1400. Where possible, data at the same level were collected with the aircraft flying directly toward the sun and then on an opposite heading to compensate for bias due to azimuth and elevation. Data were ordinarily collected above the stratus deck and then beneath it before legs were flown into the cloud layer itself in order to minimize instrument icing. Flight legs outside of the cloud were seldom more than 120 m above or below the cloud surface, so that the cloud layer essentially filled the entire field of view of the lower pyranometers on legs over the cloud and of the upper pyranometers on legs under the cloud.

b. Instrumentation

Solar radiation was measured with Eppley Precision Spectral Pyranometers (see, e.g., Coulson, 1975, p. 108) mounted on the top and bottom of the aircraft fuselage (Kelley and Zrubek, 1973). These hemispheric radiometers were equipped with Schott (Ångström and Drummond, 1961) colored filters WG-7, OG-1 and RG-8 having lower wavelength cutoffs at approximately 0.29, 0.53 and 0.68 μm, respectively. Although the NCAR pyranometers were not temperature compensated during these flights, the Eppley Laboratory has indicated that the relative sensitivity of the NCAR pyranometers varied by less than 1% over the temperature range −20 to 50°C. The boundary layer flights described here were ordinarily within this temperature range. Deviation from Lambertian cosine response was <1% over the range of zenith angles encountered. Radiometer calibrations were rechecked at NCAR in December of 1974 and in August 1976, and in an extreme case (lower RG-8) the sensitivity had changed by 2%. This analysis is concerned with flux ratios rather than absolute values of the radiance, so no empirical correction for possible absorption by the Schott filters as suggested by Drummond and Roche (1965) is made.

3. Data reduction

Raw output voltages stored on the aircraft data system were converted to radiances by the NCAR Data Management Group using a standard calibration provided by the Eppley Laboratory. Several steps were required before useful radiances could be inferred from the data provided by NCAR. First, the radiometer offset was subtracted from each radiance value based on the periodic (10 min) self-zeroing of the pyranometers during flight. This correction was generally several watts per square meter or less. Second, the downward radiance above the cloud was corrected for the nonhorizontal orientation of the pyranometers due to aircraft pitch and roll. If a right-handed coordinate system is assumed and all angles are defined as positive in the counterclockwise direction, it is straightforward to show that F^-, which is the downward flux component on a surface whose normal is the local vertical, is related to F_0^-, which is the downward flux component on a surface whose normal has arbitrary inclination, according to

$$F^- = F_0^- \left[\frac{\cos\theta}{\cos\theta \cos p \cos r + \sin\theta (\sin A \sin r - \cos A \cos r \sin p)} \right], \tag{1}$$

where p and r are the aircraft pitch and roll, respectively, A the angle between the compass direction of the sun and the aircraft true heading and θ the solar zenith angle. Except for the data collected during aircraft climbing or banking maneuvers, which were summarily discarded, the correction for pitch and roll did not exceed a few percent. No corrections were necessary for measurements of diffuse radiation, i.e., upward radiation from the cloud or ice surface, or downward radiation in or beneath the cloud.

The stratus measurements were actually taken in a moving coordinate system since the geographic location of cloud elements changed continually during the experiment due to advection. To reconstruct vertical profiles of radiometric quantities it was necessary to assume that the shape of the stratus decks did not undergo significant distortion during the course of a profile. For the analysis, cloud masses at a location $\mathbf{x}$ at time t were transformed to a fixed coordinate system $\mathbf{x}'$ according to

$$\mathbf{x}' = \mathbf{x} - \mathbf{u}(t - t_0), \tag{2}$$

where $\mathbf{u}$ was the mean wind velocity at cloud top and t_0 the time when a profile began. While some uncertainty is associated with spatial variance of $\mathbf{u}$, errors are small due to the relatively short duration of flight legs.

Radiance data from legs at a fixed level were seldom uniform due most importantly to horizontal variation of vertical cloud thickness. Since there was no means of monitoring the actual small-scale thickness variation during a flight leg, it was decided simply to compute mean values of the radiance over 1–3 min (7–20 km) intervals. "Profiles" were then reconstructed from the mean values obtained at several levels.

It was difficult to estimate cloud geometry in these experiments. Since the available (Johnson-Williams) liquid water detector could not resolve the small

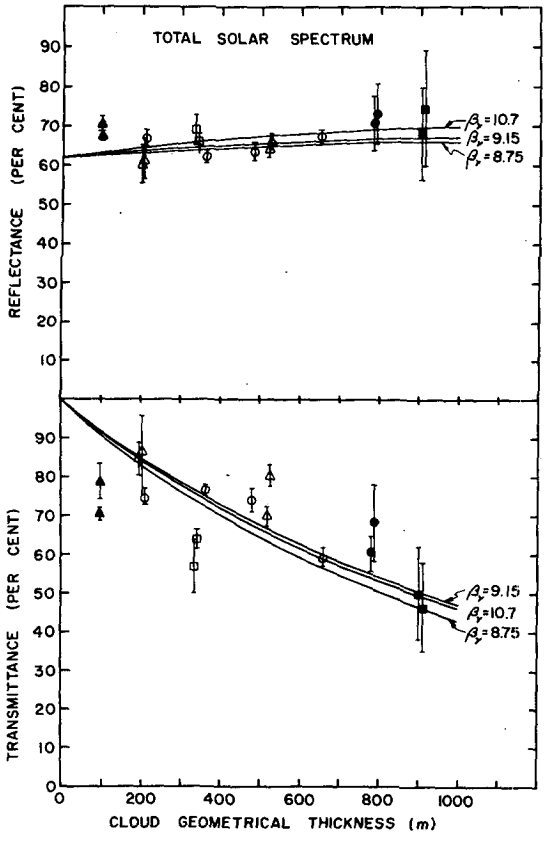

FIG. 2. Reflectance and transmittance in the spectral region 0.29–2.8 μm. In Figs. 2–5, we indicate profiles with the following geometric figures: Profile A, ▲; profile B, △; profile C, ■; profile D, ○; profile E, ●; profile F, □. Solid line denotes fit obtained with two-stream approximation for range of β_ν.

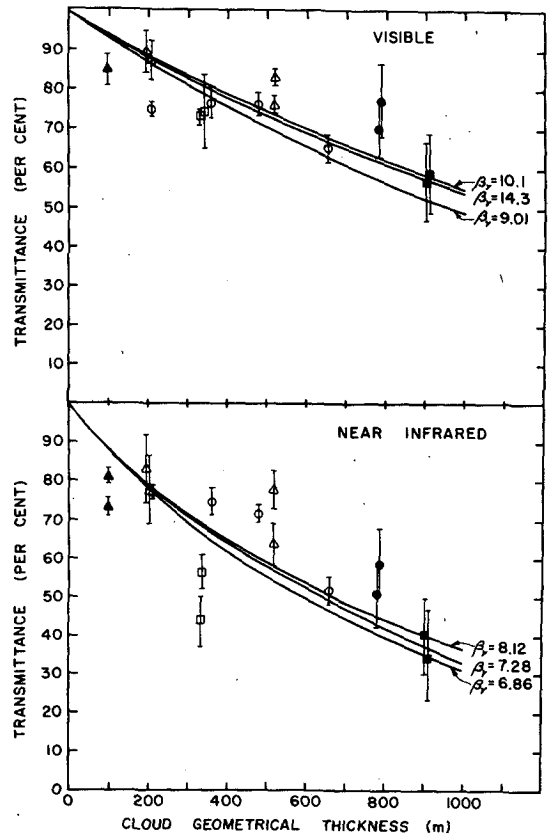

FIG. 3. Transmittance in the visible (0.29–0.68 μm) and in the near-infrared (0.68–2.8 μm). Solid line denotes fit to two-stream approximation.

water content of Arctic stratus, we relied most heavily on notes of visual observations for the location of tops and bases, which were checked by careful examination of photos from the aircraft side-looking cameras together with data from the pressure and geometric-radio altimeters. Tops were frequently characterized by 10–30 m turret elements, for which a mean height was assumed. In one case (profile D) a sloping cloud deck was encountered, and a contour flight was conducted to establish the geometry of the upper surface. Bases were notably more difficult to estimate due to the lack of visual contrast under the cloud, and the presence of 10–20 m "scud" elements protruding from the cloud bottom.

4. Results and discussion

a. Reflectance and transmittance

We let F_ν^- and F_ν^+ denote the downward and upward fluxes of hemispheric radiation, respectively. The subscript ν refers to spectral interval, which may include total solar radiation (0.29–2.8 μm), visible radiation (0.29–0.68 μm) and near-infrared radiation (0.68–2.8 μm). Total solar and near-infrared radiation are measured directly, and visible radiation is computed as their difference.

The reflectance R_ν of the *cloud plus surface system* is the ratio of the upward and downward fluxes at cloud top (z_T), and the transmittance T_ν is the ratio of the downward fluxes at cloud top and cloud base (z_B):

$$R_\nu = F_\nu^+(z_T)/F_\nu^-(z_T), \tag{3}$$

$$T_\nu = F_\nu^-(z_B)/F_\nu^-(z_T). \tag{4}$$

There is an important distinction between the optical properties of the cloud and the properties of the cloud system which consists of cloud droplets embedded in an absorbing water vapor gas and overlying a surface with a variable reflectivity. The true cloud reflective and transmissive properties are defined for a cloud over a perfectly black surface and in the absence of gaseous absorption. Without *a priori* information about the optical properties of the cloud droplets it is not possible to differentiate between the upwelling flux from the surface and that due to cloud scattering.

Above the stratus deck F_ν^- consists almost entirely of direct solar radiation, with a larger diffuse component in and beneath the cloud layer. The reflectance is the more reliable quantity since it is computed

directly from the simultaneous measurements of the upper and lower pyranometers at a fixed point. The transmittance is less reliable since there is no means of determining whether cloud optical properties or geometry changed significantly between passes at cloud top and cloud base.

Transmittances and reflectances as a function of cloud geometrical depth are shown in Figs. 2–4. (The curves represent empirical fits that are discussed in Section 4c.) The most striking feature of the reflectances in all three spectral regions is their nearly constant value with respect to the cloud thickness: total solar, 60–75%; visible, 70–85%; near-infrared, 50–65%. The importance of the surface reflected radiation is illustrated clearly when the results for Arctic stratus over ice are compared with those for marine stratus over ocean (Neiburger, 1949; Paltridge, 1974). Whereas low reflectances are observed for tenuous stratus over oceans, they appear higher over ice because the surface is so much brighter. Near-infrared reflectance values are notably smaller than visible for all cloud thicknesses since more gaseous and particulate absorption occurs in the near-infrared than in the visible. The asymptotic value of the reflectance in the limit of zero cloud thickness differs slightly from the surface albedo (see below) since it includes contributions from fog or haze which may be found between cloud base and the surface. The error bars in Figs. 2–4 indicate only the standard deviations of the reflectances and transmittances computed for the flight leg intervals (1–3 min) and do not include the instrumental error of the Eppley pyranometers.

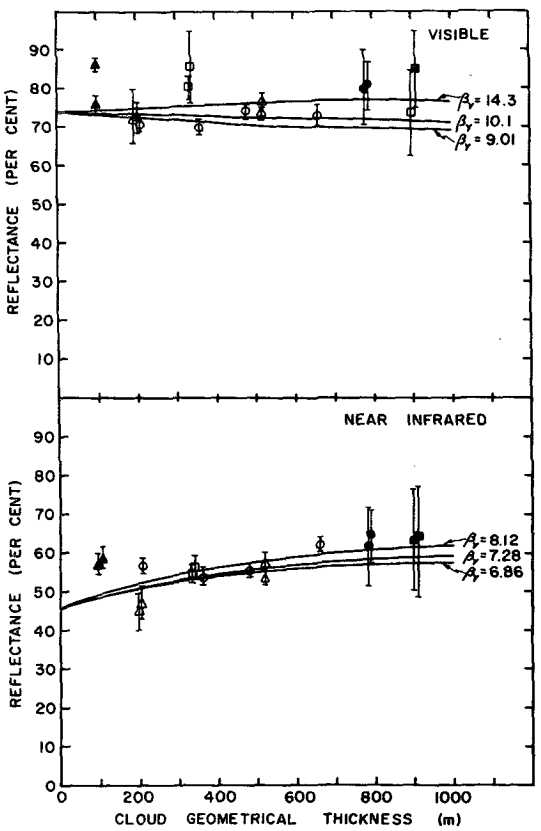

FIG. 4. Reflectance in the visible and near-infrared. Solid line denotes fit to two-stream approximation.

TABLE 2. Observations of solar absorption in stratus clouds.

Investigator	Absorption (%)	Comment
Neiburger (1949)	7	Average of all observations
Robinson (1958)	19	Average of all stratiform cloud
Koptev and Voskresenskii (1962)	4–10	Range for 200–500 m st
Griggs (1968)	4	Average of all observations
Paltridge (1971)	0	Average of three sc decks
Reynolds *et al.* (1975)	23	Average of three sc decks

These reflectivities are in good agreement with those calculated theoretically by Wiscombe (1973, Table III). He obtains $R_v=0.681$ for a solar elevation of 30° and a surface reflectivity of 0.58.

The surface effect is also evident in our calculations of transmittance. Comparing our results with Neiburger's Fig. 4, one finds, for example, that the transmittance in a 600 m Arctic stratus cloud is 60%, but only 20% in California stratus. Transmittances decrease more rapidly with cloud thickness in the near-infrared than in the visible due to greater absorption in the nir.

b. Absorptance

The combined gaseous and droplet absorptance in a cloud layer is

$$A_v=\frac{F^-(z_T)+F^+(z_B)-F^-(z_B)-F^+(z_T)}{F^-(z_T)}. \quad (5)$$

While it has been a straightforward matter to measure the fluxes on the right-hand side of (5) in previous experiments, there still seems to be some uncertainty about how much radiation stratus layers actually absorb. Table 2, which summarizes a number of stratus measurements, illustrates this point well. The calculated absorptances vary widely because they are computed as the relatively small difference of four fluxes that are themselves difficult to measure precisely. The cumulative effect of error sources such as cloud inhomogeneity combine to produce large standard deviations, and in some cases negative absorptances. In fact when (5) was applied to the data described here negative absorptances were obtained for 10% of the values in the total spectrum, 20% in the visible, and 17% in the near-infrared. Table 3

TABLE 3. Average absorptance in stratus cloud layers (percent).

Flight leg	Total solar	Visible	Near-infrared
A	11±3	6±5	5± 3
B	6±6	3±6	9± 6
C	12±9	6±9	18±10
D	3±2	4±3	2± 1
E	6±8	3±7	9±10
F	9±5	0±6	11± 5
All flights	7±8%	5±8%	9± 9%

summarizes the average absorptances for flight legs A–F. The average for all flights suggests an upper bound for absorptance of roughly 7, 5 and 9% for the total, visible and near-infrared spectra, respectively. Despite the rather large relative error in the absorptance values, Table 3 illustrates the important feature that the water vapor and droplets in a stratus layer absorbed substantially more solar radiation in the near infrared part of the spectrum than in the visible.

c. *Derived quantities*

Reflectance, transmittance and absorptance are bulk properties of the cloud-surface system and are computed in a straightforward manner. What other information about the stratus layer can be deduced from these few flight legs? Radiometer observations yield an upward (F_ν^+) and downward (F_ν^-) flux above and beneath the cloud layer and frequently at several levels in the cloud itself. The upward flux at cloud top and downward flux at cloud base together with ground albedo in principle determine two parameters in a radiation model. Fluxes at additional levels may be used to determine additional parameters.

This analysis fits the observed upward and downward fluxes to Chandrasekhar's (1960) *first approximation* to determine the single-scattering albedo $\tilde{\omega}_\nu$ and the absorption optical depth τ_ν. (The flux equations in the first approximation are cumbrous and are given in the Appendix.)

Letting s_ν and $k_{c\nu}$ denote the frequency dependent volume scattering and absorption coefficients, respectively, and $k_{g\nu}$ the gaseous absorption coefficient, the extinction optical depth is

$$\tau_\nu' = \int_z^\infty (s_\nu + k_{c\nu} + k_{g\nu})\,dz \tag{6}$$

and the single-scattering albedo

$$\tilde{\omega}_\nu = \frac{s_\nu}{s_\nu + k_{g\nu} + k_{c\nu}}. \tag{7}$$

The absorption optical depth is defined by

$$d\tau_\nu = (1-\tilde{\omega}_\nu)\,d\tau_\nu'. \tag{8}$$

In this variant of a two-stream approximation two measures of the particle's phase function are retained, namely $\tilde{\omega}_\nu$ and the asymmetry factor $\langle\cos\theta\rangle$. The quantity $\tilde{\omega}_\nu\langle\cos\theta\rangle$ is the only measure of isotropy, and $\langle\cos\theta\rangle = 1$ for fully forward scattering and is zero for isotropic scattering. This analysis does not deduce the factor $\langle\cos\theta\rangle$ since it appears to have a relatively constant value near 0.85 in the frequency and particle size regimes considered here (Irvine and Pollack, 1968; Twomey, 1976). These quantities may be combined into the parameter

$$\beta_\nu^2 = \frac{3(1-\tilde{\omega}_\nu\langle\cos\theta\rangle)}{(1-\tilde{\omega}_\nu)}, \tag{9}$$

where β_ν is a measure of the increase of absorption path length caused by multiple scattering when a photon traverses a fixed distance.

The absorption optical depth τ_ν is estimated by fitting the observed upward and downward fluxes to (A9) and (A10) with a standard nonlinear least-squares regression. Average fluxes were weighted according to the cube of their standard deviation. Where there was more than one vertical profile in a single cloud layer the data were combined and the fit was applied to the entire set of upward and downward fluxes. Optical depths as function of cloud thickness are determined for all six cloud profiles are shown together in Fig. 5. There is obviously much scatter in these data, and this illustrates well the difficulty of measuring clouds that are not horizontally homogeneous or overlying a surface of nonuniform albedo. However, a range and trend is evident. Because we require an approximate relation between absorption optical depth and cloud thickness a linear regression is computed for these points. This is a probable oversimplification in view of Neiburger's (1949) and Paltridge's (1974) observations of the height variation of cloud liquid water in marine stratus. (Liquid water was not measured in the flights described here.) The best linear fits to the points in each spectral region are shown by the dashed lines in Fig. 5, while the neighboring lines represent 95% confidence limits. The data scatter simply does not justify fitting a more complicated function.

The scattering parameter β_ν is calculated by fitting the complete set of reflectances and transmittances to Eqs. (3), (4), (A9) and (A10) and using the assumed linear relation between τ_ν and the observed cloud thickness Δz. Because reflectance is an intrinsically better measurement of a true cloud property, reflectance and transmittance data are weighted in the ratio 2:1. These results are presented in Table 4, where $\partial\tau_\nu/\partial(\Delta z)$ refers to the best linear fit of τ_ν as a function of Δz, β_ν is the best fit to the observed reflectances and transmittances, and $\tilde{\omega}_\nu$ is the single scattering albedo computed from β_ν by assuming an asymmetry factor of 0.85. The range of β_ν and $\tilde{\omega}_\nu$

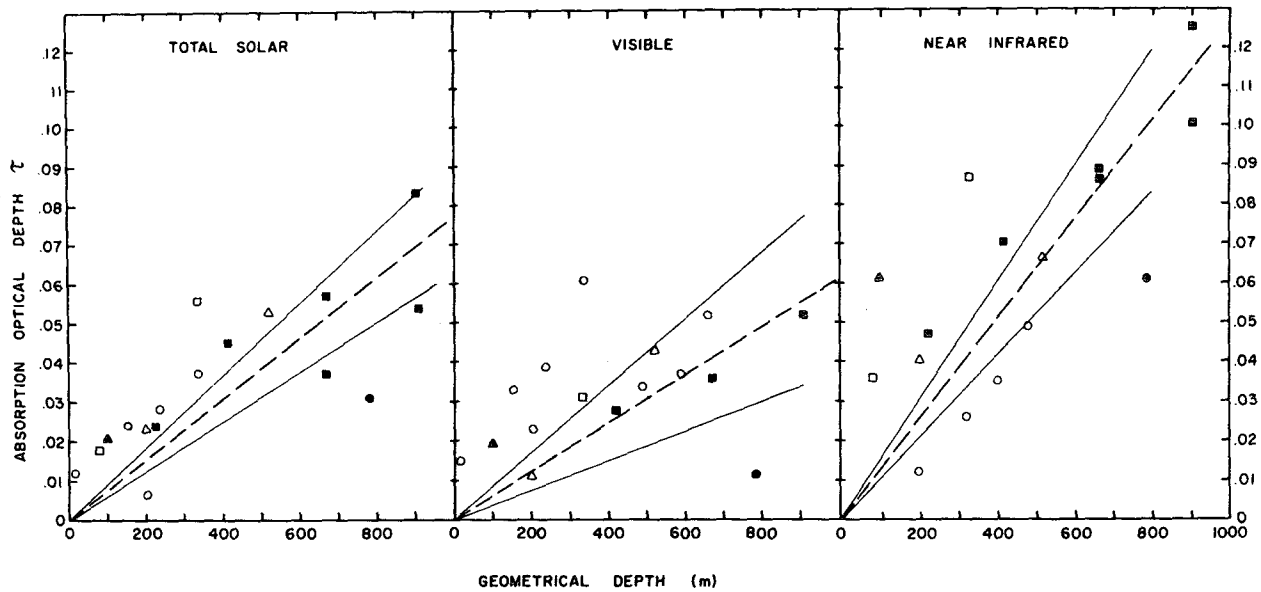

FIG. 5 Absorption optical depth determined by fitting flux profiles to two-stream approximation. Broken line denotes a linear regression through these points, while solid lines denote 95% confidence limits.

refers to values calculated with the 95% confidence values of $\partial\tau_\nu/\partial(\Delta z)$.

The absorption optical depths presented in Fig. 5 are converted to extinction optical depths by dividing by $(1-\tilde{\omega}_\nu)$. For example, the extinction optical depths in a 500 m cloud are total solar spectrum, 7.0; visible, 6.9; near-infrared, 7.1.

The range of β_ν for the total spectrum compares favorably with the Mie theory values used in the Herman and Goody (1976) stratus model. From their Table 1 one finds for a droplet density of 5×10^7 m^{-3} and a mean radius of 6.5 μm that $\beta_\nu=7.6$ in the "weak" region of the spectrum, assuming a water vapor mixing ratio of 3×10^{-3}.

With these inferred values of β_ν, or alternatively, the single scattering albedo, it is possible to estimate the absorption (see Fig. 6) for clouds of varying geometrical thickness using (A9) and (A10). One obtains in a 500 m cloud, for example, total solar, 8.5%; near-infrared, 12.6%; visible, 7.7%. These values are not inconsistent with the absorptance values computed with the bulk absorptance formula (5), or with the values determined by the investigators listed in Table 2. And to the extent that the first approximation is an adequate means of specifying solar radiation in stratus layers, it seems that this approach provides a reliable estimate of bulk absorptance by utilizing the very large sample in its nonlinear least-squares fit of data collected during all legs of all flights.

It remains difficult, however, to reconcile the large absorptances inferred here and in most stratus experiments conducted over the past two decades with the smaller absorptances suggested by theoretical calculations. Twomey (1976), for example, has presented theoretical calculations of single scatter albedo as a function of wavelength. The present near-infrared values of $0.990<\tilde{\omega}_\nu<0.993$ would agree well with a weighted mean of Twomey's values in this spectral region. On the other hand we find $0.994<\tilde{\omega}_\nu<0.998$ in the visible, while Twomey's calculations yield $0.999<\tilde{\omega}_\nu<0.99999$ at wavelength <0.7 μm. What may possibly be the reason for this discrepancy? There

TABLE 4. Derived scattering parameters.

Region	$\partial\tau_\nu/\partial(\Delta z)$ (m^{-1})	β_ν	Range	$\tilde{\omega}_\nu$	Range
Total solar spectrum	7.73×10^{-5}	9.15	8.75–10.7	0.995	0.994–0.996
Visible	6.17×10^{-5}	10.1	9.01–14.3	0.996	0.994–0.998
Near infrared	1.26×10^{-4}	7.28	6.86–8.12	0.991	0.990–0.993

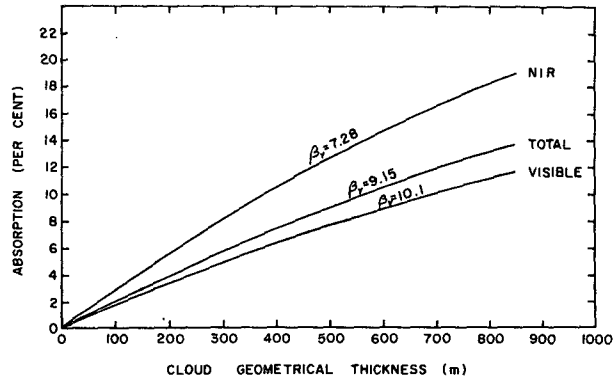

FIG. 6. Absorption computed with the first approximation, using derived values of β_ν. NIR = near-infrared.

TABLE 5. Spatially averaged surface albedo.

Profile	Total solar	Visible	Near-infrared
B	0.63±0.08	0.75±0.09	0.46±0.05
C	0.64±0.05	0.73±0.08	0.49±0.03
D	0.53±0.03	0.66±0.02	0.38±0.02
E	0.56±0.04	0.68±0.04	0.38±0.03
F	0.54±0.02	0.66±0.02	0.37±0.02
All flights	0.58±0.05	0.70±0.06	0.42±0.03

is some slight liquid water absorption in the visible (see, e.g., Goody, 1964, Appendix 13), but it is certainly too small to account for the difference. Twomey's (1972) calculations further discount the possibility of aerosol absorption in clouds. It is becoming more plausible that some of the observed absorption may actually be lateral exchange at the edge of the stratus deck (Davies, 1976). Edge effects may have been important in some flights since they were frequently relatively close ($\lesssim 20$ km) to the deck limits to maintain cloud identity. The values in the visible also contain combined errors in the total solar and near-infrared measurements since visible fluxes were computed as their difference.

d. *Surface Albedo*

Flight legs that were conducted at altitudes of 100 m or less yield values of the areally averaged surface albedo α_ν. Although the radiometers sensed diverse surface elements such as frozen and open meltwater ponds, ice and snow in various stages of melting, and open leads, fast (1 s) data collection rates allow 10–40 km averages to be calculated. These spatial averages, which are ultimately more useful for energy budget or bulk radiative transfer calculations, are presented in Table 5. These albedo values refer to overcast conditions only, i.e., they are albedos for the diffuse radiation field. While these values do not differ markedly from other observations in the central Arctic (Chernigovskii, 1963) they do illustrate the important difference between visible and near-infrared reflectances of the surface: The pack ice absorbs a larger (28%) fraction of radiation in the near-infrared than it does in the visible.

5. Remarks

The measurements described here illustrate a number of important features of Arctic stratus clouds. Over the range of solar elevations and surface ice conditions typical of the Beaufort Sea in summer we have estimated the relation between cloud thickness and transmittance, and have observed relatively constant values of the cloud reflectance. Bulk absorptance remains, at best, ambiguous. Plausible ranges for the single scattering albedo and absorption optical depth are estimated from a two-stream approximation for a plane parallel cloud layer with assumed droplet homogeneity.

Observational studies of stratus layers have rather consistently yielded absorptances in the range of 5–10%, but with large relative error. These values most frequently obtain from bulk formulas such as Eq. (5), and are supported by alternative analyses such as presented here. Are these large absorptances real, or are they caused by instrumental deficiencies, or a three-dimensional effect? The ideal plane-parallel and homogeneous conditions are seldom realized, and hemispheric pyranometers may perhaps be somewhat inadequate for accurately determining fluxes in complicated cloud situations. Clearly, more sophisticated radiometric techniques are required to resolve the cloud absorptance question.

Acknowledgments. It is a pleasure to acknowledge the support and assistance during the course of this program of numerous individuals from the NCAR Research Aviation Facility, the Arctic Ice Dynamics Joint Experiment and the Space Science and Engineering Center. The author also appreciates the valuable comments and criticisms offered by Dr. Richard Goody. This work was supported by a subcontract from the University of Washington under National Science Foundation Grant OCD-75-19758.

APPENDIX

Chandrasekhar's "First Approximation"

The flux model to which the aircraft data are fitted is Chandrasekhar's (1960, p. 149) first approximation. This variant of the two-stream approximation represents the upward and downward intensities by two streams of radiation, denoted by I_ν^+ and I_ν^-, respectively according to

$$\frac{1}{\sqrt{3}}\frac{d}{d\tau_\nu'}(I_\nu^+ - I_\nu^-) = (1-\tilde{\omega}_\nu)(I_\nu^+ + I_\nu^-), \tag{A1}$$

$$\frac{1}{\sqrt{3}}\frac{d}{d\tau_\nu'}(I_\nu^+ + I_\nu^-) = (1-\tilde{\omega}_\nu\langle\cos\theta\rangle)(I_\nu^+ - I_\nu^-). \tag{A2}$$

When $\tilde{\omega}_\nu$ is constant with respect to τ_ν' it is straightforward to combine (A1) and (A2) by differentiation. In realistic clouds $\tilde{\omega}_\nu = \tilde{\omega}_\nu(\tau')$, i.e., the single scattering albedo varies with extinction optical depth and (A1) and (A2) are more conveniently reformulated in terms of the absorption optical depth (8). The upward flux in the first approximation is $F_\nu^+ = 2\pi I_\nu^+/\sqrt{3}$, the downward flux is $F_\nu^- = -2\pi I_\nu^-/\sqrt{3}$, and the net flux is

$$F_\nu = \frac{2\pi}{\sqrt{3}}(I_\nu^+ - I_\nu^-). \tag{A3}$$

Combining (A1)–(A3) we obtain

$$\frac{d^2F_\nu}{d\tau_\nu^2}=\beta_\nu^2F_\nu, \tag{A4}$$

where β_ν^2 is defined as in Eq. (9).

At the lower boundary ($\tau_\nu=\tau_\nu^*$) with surface albedo α_ν the boundary condition is $I_\nu^+=\alpha_\nu I_\nu^-$ so that

$$\frac{dF_\nu}{d\tau_\nu}+\sqrt{3}\left(\frac{1+\alpha_\nu}{1-\alpha_\nu}\right)F_\nu=0 \quad \text{at} \quad \tau_\nu=\tau_\nu^*. \tag{A5}$$

The direct solar beam is a boundary condition at $\tau_\nu=0$:

$$2\pi I_\nu^-=\sqrt{3}\mu_0 f_\nu, \tag{A6}$$

where f_ν is the solar irradiation at cloud top and μ_0 the cosine of the solar zenith angle. At the cloud top

$$\frac{dF_\nu}{d\tau_\nu}-\sqrt{3}F_\nu=2\sqrt{3}\mu_0 f_\nu \quad \text{at} \quad \tau_\nu=0. \tag{A7}$$

In a homogeneous atmosphere, where the coefficient β_ν^2 would be effectively constant, the solution to (A4) is exponential, i.e.,

$$F_\nu=C_1\exp(+\beta_\nu\tau_\nu)+C_2\exp(-\beta_\nu\tau_\nu). \tag{A8}$$

The coefficients C_1 and C_2 are determined by the boundary conditions at $\tau_\nu=0$ and $\tau_\nu=\tau_\nu^*$, and expressions for them are given elsewhere (Herman and Goody, 1976, Appendix B). From (A3) the upward and downward fluxes are found to be

$$F_\nu^+=\tfrac{1}{2}[C_1\exp(+\beta_\nu\tau_\nu)(1+\beta_\nu/\sqrt{3}) +C_2\exp(-\beta_\nu\tau_\nu)(1-\beta_\nu/\sqrt{3})], \tag{A9}$$

$$F_\nu^-=\tfrac{1}{2}[C_1\exp(+\beta_\nu\tau_\nu)(1-\beta_\nu/\sqrt{3}) +C_2\exp(-\beta_\nu\tau_\nu)(1+\beta_\nu/\sqrt{3})]. \tag{A10}$$

Eqs. (A9) and (A10) express the upward and downward flux as a function of three quantities: asymmetry factor $\langle\cos\theta\rangle$, single scattering albedo $\tilde{\omega}_\nu$ and absorption optical depth τ_ν. These relatively straightforward flux equations apply strictly to a homogeneous cloud layer. In an ideal aircraft experiment there would be a sufficient number of flight levels in the cloud to allow solutions of (A9) and (A10) within each discrete layer. This is ordinarily not feasible due to the realities of cloud geometry and aircraft cost, and in fact only a few legs (cf. Fig. 1) are possible in each cloud layer. It therefore becomes necessary to treat as homogeneous some cloud layers whose drop size and liquid may vary somewhat over the depth of the layer.

It does not seem, however, that we incur a serious error in treating the cloud strata as homogeneous slabs, because the effect of varying droplet densities becomes insignificant in regions of the spectrum when there is strong particle absorption. From Herman and Goody's (1976) approximations for volume scattering and absorption coefficients we have

$$\frac{\beta_\nu^2}{3}=1+\frac{\overline{Q_s^S}(1-\langle\cos\theta\rangle)}{\overline{Q_a^S}+(k_g/N_0\pi a^2)}, \tag{A11}$$

where $\overline{Q_s^S}$ and $\overline{Q_a^S}$ are scattering and absorption efficiencies computed from Mie theory, N_0 is the droplet density, a the mean droplet radius and k_g the volume absorption coefficient for the gas. Provided that the droplet size spectrum remains relatively constant with height, Eq. (A11) indicates that variations of β_ν^2 are associated with variations of the quantity $k_g/N_0\pi a^2$. Typically $\overline{Q_a^S}\sim0.01$, $a\sim6.5$ μm and $N_0\sim10^8$ m^{-3}. For visible radiation $k_g/N_0\pi a^2\ll\overline{Q_a^S}$ and β_ν^2 is effectively constant. For near-infrared radiation $k_g/N_0\pi a^2<Q_a^S$ in the "transparent" region (Herman and Goody, 1976, p. 1540), or alternatively, in the interband gaps (Feigel'son, 1964, Table 1.4.21). Only in tenuous clouds at water vapor band centers will β_ν^2 vary significantly. In fact, the derived values of β_ν^2 indicate *a posteriori* a regime of strong particle absorption. We therefore assume that constancy of β_ν^2 holds to a good approximation for the purposes of this analysis.

REFERENCES

Ångström, A. K., and A. J. Drummond, 1961: Basic concepts concerning cutoff glass filters used in radiation measurements. *J. Meteor.*, 18, 360–367.

Chandrasekhar, S., 1960: *Radiative Transfer*. Dover, 393 pp.

Chernigovskii, N. T., 1963: Radiational properties of the central Arctic ice coat. *Tr. Ark. Antark. Nauchno-Issled. Inst.*, 253, 249–260.

Coulson, K. L., 1975: *Solar and Terrestrial Radiation*. Academic Press, 322 pp.

Davies, R., 1976: The three dimensional transfer of solar radiation in clouds. Ph.D. thesis, University of Wisconsin, 200 pp.

Drummond, A. J., and J. J. Roche, 1965: Corrections to be applied to measurements made with Eppley (and other) spectral radiometers when used with Schott colored glass filters. *J. Appl. Meteor.*, 4, 741–744.

Feigel'son, E. M., 1964: *Light and Heat Radiation in Stratus Clouds*. Izv. "Nauka," 245 pp. [English translation by Israel Program for Scientific Translation, 1966.]

Gavrilova, M. K., 1963: *Radiation Climate of the Arctic*. Leningrad, Gidrometeor., 178 pp. [English translation by Israel Program for Scientific Translation, 1966.]

Goody, R. M., 1964: *Atmospheric Radiation*. Clarendon Press, 436 pp.

Griggs, M., 1968: Aircraft measurements of albedo and absorption of stratus clouds, and surface albedos. *J. Appl. Meteor.*, 7, 1012–1017.

Herman, G., and R. Goody, 1976: Formation and persistence of summertime Arctic stratus clouds. *J. Atmos. Sci.*, 33, 1537–1553.

Irvine, W. M., and J. B. Pollack, 1968: Infrared optical properties of water and ice spheres. *Icarus*, 8, 324–360.

Kelley, N. D., and M. N. Zrubek, 1973: Instrumentation aboard the Electra. *Atmos. Tech.*, **1**, NCAR, 18–20.

Koptev, A. P., and A. I. Voskresenskii, 1962: On the radiation properties of clouds. *Tr. Ark. Antark. Nauchno-Issled. Inst.*, **239**, No. 2, 29–47.

Marshunova, M. S., 1961: Principal characteristics of the radiation balance of the underlying surface and of the atmosphere in the Arctic. *Tr. Ark. Antark. Nauchno-Issled. Inst.*, **229**, 5–53.

Neiburger, M., 1949: Reflection, absorption, and transmission of insolation by stratus cloud. *J. Meteor.*, **6**, 98–104.

Paltridge, G. W., 1974: Atmospheric radiation and the gross character of stratiform cloud. *J. Atmos. Sci.*, **31**, 244–250.

——, 1971: Solar and thermal radiation flux measurements over the east coast of Australia. *J. Geophys. Res.*, **76**, 2857–2865.

Reynolds, D. W., T. H. Vonder Haar and S. K. Cox, 1975: The effect of solar radiation absorption in the tropical troposphere. *J. Appl. Meteor.*, **14**, 433–444.

Robinson, G. D., 1958: Some observations from aircraft of surface albedo and the albedo and absorption of cloud. *Arch. Meteor. Geophys. Bioklim.*, **B9**, 28–41.

Twomey, S., 1972: The effect of cloud scattering on the absorption of solar radiation by atmospheric dust. *J. Atmos. Sci.*, **29**, 1156–1159.

——, 1976: Computations of the absorption of solar radiation by clouds. *J. Atmos. Sci.*, **33**, 1087–1091.

Vowinckel, E., and S. Orvig, 1962: Relation between solar radiation income and cloud type in the Arctic. *J. Appl. Meteor.*, **1**, 552–559.

——, and ——, 1970: The climate of the North Polar Basin. *World Survey of Climatology*, Vol. 14, *Climates of the Polar Regions*, S. Orvig Ed., Elsevier, 370 pp.

Wiscombe, W. J., 1973: Solar radiation calculations for arctic summer stratus conditions. *Climate of the Arctic*, S. A. Bowling and G. Weller, Eds., Geophysical Institute, University of Alaska, 238–244.